Desalination and Water Treatment
www.deswater.com

doi: 10.1080/19443994.2015.1091990

57 (2016) 18326–18337
August

Taylor & Francis
Taylor & Francis Group

Potential of environmental-friendly, agro-based material *Strychnos potatorum*, as an adsorbent, in the treatment of paint industry effluent

S. Vishali[a,*], P. Rashmi[a], R. Karthikeyan[b]

[a]*Department of Chemical Engineering, SRM University, Chennai 603 203, India, Tel. +91 94438 83562; email: meet.vishali@gmail.com (S. Vishali), Tel. +91 9743749703; email: rashmi_p30@yahoo.com (P. Rashmi)*
[b]*AAMEC, Thanjavur 614 403, India, Tel. +91 9940561915; email: drrkarthi@yahoo.com*

Received 16 February 2015; Accepted 23 August 2015

ABSTRACT

The study was focused on, to make use of the agro-based material *Strychnos potatorum* as an adsorbent, for the treatment of simulated water-based paint industry effluent (PIE) in a fixed-bed adsorption column (FBC). The influence of bed height, flow rate, and initial concentration of PIE were evaluated in terms of color removal efficiency. The highest color removal was achieved at a larger breakthrough time, and lengthier mass transfer zone was viewed at the lowest flow rate, lowest initial concentration, and highest bed height used in this study. For a successful design of a FBC, breakthrough curves were made and the experimental data were fitted using well-established models such as: Thomas/Bed depth service time (BDST), Adams–Bohart, Yoon–Nelson, and Wang. From the plot of these models, parameters like adsorption capacity and rate constants were calculated. Mass transfer models like Weber–Morris, Boyd, Urano–Tachkawa, and Mathews–Weber were applied to identify the rate-limiting step of the overall adsorption process. All the model parameter values, which are the basis for the process design at a real scale were calculated. On the basis of the results obtained in this study, it was suggested that the agro-based material *S. potatorum*, affirmed its positive potentiality and could be used economically and effectively, as an adsorbent in the treatment of hazardous PIE.

Keywords: *S. potatorum*; Paint industry effluent; Fixed-bed column; Adsorption; Mass transfer models

1. Introduction

Paint is normally a mixture of pigment, binder, solvent, and additives. From the environment and treatment point of view, one convenient way to classify paint is on the basis of their primary solvent. According to this method, paints can be classified as water-based, organic solvent-based or powder (dry), and without solvent. The wastewater generated from the paint industry is mainly by the cleaning operations of mixers, reactors, blenders, filling lines, packing machines, and floor [1]. The discharge of such polluted effluents into the environment damages the quality of the receiving stream, aquatic life, and enhances the toxicity. In order to respect the environment and the law, the generated wastewater is to be treated prior to disposal [2].

Researchers have reported the treatment of paint industry effluent (PIE) by various methods, such as

*Corresponding author.

physical–chemical treatment [3], bio oxidation [4], biological treatment [5], activated sludge treatment [6], micro filtration [7], coagulation–flocculation processes [8], Fenton oxidation [9], adsorption [10], electrochemical oxidation [11], and electro coagulation [12].

Biosorption is an improving and proven eco-friendly technology for the removal of color, and heavy metals from water and wastewater. This technology has several advantages, such as, simplicity of design, ease of operation, insensitivity to toxic substances, and complete removal of pollutants even from dilute solutions [13].

Also this method will become inexpensive, if the sorbent material used is of cheaper cost and does not require any expensive additional pre-treatment step. Successful treatment of wastewater not only depends on the pollutant removal ability of the material, but also requires an abundance of the material for the purpose. It follows therefore that the adsorbent should either be an industrial waste product or one that is available plenty in nature [14]. *Strychnos potatorum*, also known as clearing-nut tree, grows in southern and central parts of India, Sri Lanka, and Burma. Sanskrit writings from India report that the seeds were used to clarify turbid surface water over 4,000 years ago [15]. Due to their natural abundance and affinity for color, *S. potatorum* seeds stay a cheap and readily available source of bioadsorbent.

By reviewing the literature, it was observed that *S. potatorum* seeds were used as a natural coagulant to clarify turbid water [16,17], and as an adsorbent to remove heavy metals from aqueous solution [18,19]. The efficacy of the seeds was not examined for the treatment of any industrial effluent. It was also seen that no attempt has been made so far to use agro-based materials as an immobilized adsorbent in the removal of color from PIE.

Keeping this in view, this study was aimed to investigate the feasibility of using *S. potatorum* seeds as an efficient adsorbent for the removal of color from PIE by varying the operational parameters, such as flow rate, bed height, and effluent initial concentration.

2. Materials and methods

2.1. Materials

2.1.1. Adsorbate

All the chemicals used in the experiments were of analytical grade. The simulated water-based PIE was prepared by adding different proportions of commercially available white primer and an acrylic-based blue colorant and made up to 1,000 mL, using double-distilled water (5% (v/v)) [11]. Three different samples were prepared and named as sample numbers 1–3 (Table 1). The physical–chemical properties of the simulated PIE (sample 3), which resembled the real effluent from paint industry, are listed in Table 2.

2.1.2. Agro-based adsorbent

The seeds of *S. potatorum* were collected from Thirumayam, a rural area in Pudukottai district, South India. The seeds were washed thoroughly with deionized water, sun-dried for 48 h, powdered, and sieved through 0.5-mm sieve (Fig. 1).

2.1.3 Fixed-bed column

A fixed-bed column made up of Pyrex glass with an inner diameter 2 cm and length 50 cm with tapered end was designed and fabricated for lab facility, to conduct the continuous adsorption process (Fig. 2). The effluent was introduced into the FBC, using a peristaltic pump (Ravel Hitek, India) at a room temperature of 30˚C.

2.2. Methods

2.2.1. Preparation of immobilized beads

For the immobilization of *S. potatorum* adsorbent, sodium alginate was used as a matrix. The powdered material (3% (w/v)) and sodium alginate (1% (w/v)) were suspended in distilled water. This suspension was stirred using magnetic stirrer with hot plate for about 15 min. The temperature was maintained within 45˚C, in order to avoid the loss of adsorption properties of the adsorbent. The resultant slurry was extruded as a drop in sterile 3% $CaCl_2$ solution at room temperature, using a syringe. The beads were hardened by resuspending in a fresh $CaCl_2$ solution for 24 h at 4˚C, and finally these beads were washed with deionized water to remove excess calcium ions [20]. Immobilized beads without the addition of natural materials were used as a control (Fig. 1).

2.2.2. Experimental setup

A fixed-bed column (FBC) was placed with glass wool in the bottom. Immobilized beads of *S. potatorum* were packed in the column to the desired height, between two supporting layers of glass beads. A final layer of glass beads was placed at the top to provide a uniform inlet flow. The presence of glass wool at the

Table 1
Concentration of simulated PIE samples (made up to 1,000 mL)

Sample number	White primer (mL)	Blue colorant (mL)	Initial COD (mg/L)
1	48	2	3,100
2	44	6	5,650
3	40	10	7,693

Table 2
Physicochemical characteristics of the simulated PIE (Sample number 3)

Parameters	Concentration (except for pH, color and turbidity)
pH at 25°C	7.6
Color (nm)	0.4583
Total dissolved solids (mg/L)	304
Total suspended solids (mg/L)	6,880
Oil and grease (mg/L)	19
Chloride as Cl (mg/L)	68
Chemical oxygen demand (COD) (mg/L)	7,693
Sulfate as SO_4 (mg/L)	24
Biochemical oxygen demand (mg/L) (3 d incubated at 27°C)	2,648
Iron as Fe (mg/L)	0.05
Turbidity, NTU	7,760

bottom was to avoid the blockage of glass beads in the outlet. The adsorbate was introduced in a down-flow mode, using a peristaltic pump at a room temperature of 30°C without any pH adjustment.

Uniform packing of the adsorbent was ensured for every run by filling the column with deionized water, after which the beads were slowly added. Almost uniform and constant packing was achieved for each run because of the terminal settling velocity. After the required height of packing was attained, the water was drained, resulting in more compact packing. Prior to every run, the mass of the adsorbent used in the packing was noted. The treated effluent samples were collected at specific time intervals and analyzed for residual color using UV visible double spectrophotometer at 612 nm.

The column studies were terminated when the column reached exhaustion point. A FBC operation was performed isothermally at 30 ± 1°C. All the experiments were carried out at least thrice to ensure reproducibility. The reported values were the average of three data sets. A series of experiments was carried out to study the effect of flow rate (5, 10, 15 mL/min), bed height (5, 15, 25 cm), and initial concentration of PIE (3,100, 5,650, 7,693 mg/L), named as sample number 1–3, respectively.

3. Fixed-bed adsorption process analysis

The successful design of an adsorption column requires the prediction of the concentration–time profile from the breakthrough curve for the effluent discharged from the column [21]. The shape of the breakthrough curve is a very important characteristic for determining the operation and the dynamic response of an adsorption fixed-bed column. It shows the loading behavior of the color to be removed from PIE in a fixed-bed column, and is usually expressed in terms of adsorbed color concentration (C_{ad}), inlet color concentration (C_o), and outlet color concentration (C_t) [22]. All the terms used for describing the adsorption behavior of a FBC are listed in Tables 3a and 3b.

4. Results and discussions

4.1. Characterization of S. potatorum

The ability of *S. potatorum* mainly depends on the chemical reactivity of the functional groups present in it. The different chemical functional groups present in the adsorbent were observed by FTIR analysis

Fig. 1. *S. potatorum* seeds, powder, and immobilized beads Schematic diagram of fixed-bed column.

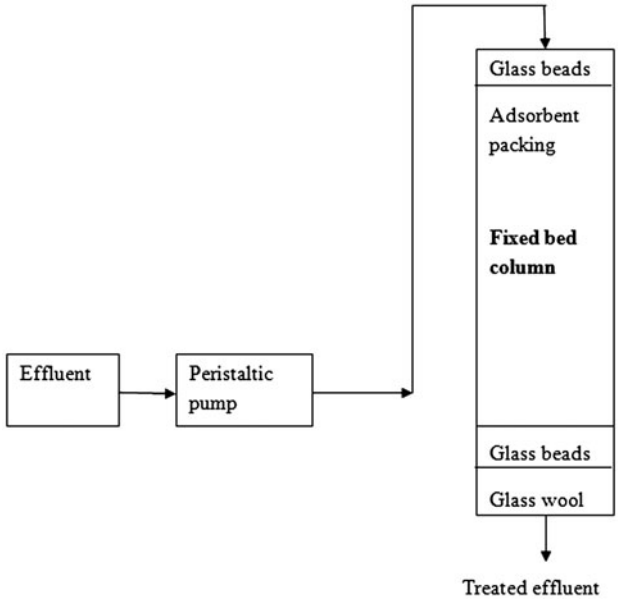

Fig. 2. Schematic diagram of a fixed-bed adsorption column (FBC).

(Fig. 3a). The intense peak at 3,417.47 cm^{-1} was due to OH stretching vibration of water and stretching vibration of amine. The presence of C–N stretching vibration was confirmed at 1,156 cm^{-1}. The presence of H_2O was also confirmed by its bending vibration at 1,651 cm^{-1}. The peak at 2,926.05 cm^{-1} was due to $-CH_2$ vibration of alkyl group. The CH_2 bending vibration occurred at 1,431 cm^{-1}. The intense peak at 1,021.48 cm^{-1} was due to –CO stretching vibration of ether groups. So, the FTIR spectra reveal that the seed mainly carries aliphatic groups with ether linkages and amine groups.

4.1.1. Identification and estimation of protein

The presence of protein in the *S. potatorum* seeds is the responsible agent for the adsorption process [23]. To confirm the presence of protein, analysis was done by SDS-PAGE and silver staining and the protein bands could be seen in Fig. 3b, with a molecular weight range of 34,000–44,000 Da. The protein concentration was estimated using Bradford Method, and the values are 79.80 and 91.80 mg/mL before and after the dialysis,respectively.

4.1.2. Characterization of S. potatorum immobilized beads

The mean diameter of the beads is calculated using volume displacement method and the value is 0.5347 cm. By measuring the weight of known number of beads, and its diameter, the bead density was calculated as 0.9 g/cc. The bulk density of the adsorbent was calculated using the ratio between the total mass of the beads used for the required packing height per volume of the beads.

4.2. Effect of operating parameters on the breakthrough curves

4.2.1. Effect of inlet flow rate

The flow rate of PIE is a major consideration when designing an adsorption column, because it has a significant effect on adsorption of color (or other pollutants) from the effluent being treated in a FBC. The effect of flow rate is shown in Fig. 4 with the help of experimental breakthrough curve. In the present study, the flow rate was varied as 5, 10, and 15 cc/min with controlled bed height and initial concentration.

As the flow rate speeded up from 5 to 15 cc/min, the breakthrough curve emerged at a comparatively faster rate, and less time was taken to reach the saturation breakthrough. The breakthrough time turned out as 361, 285, and 190 min for flow rate values of 5, 10, and 15 cc/min, respectively. The total percentage of color removal corresponding to the stoichiometric capacity of the column, declined by as much as

Table 3a
Fixed-bed adsorption process analysis parameters

Volume of effluent treated (mL)	$V_{\text{eff}} = Qt_t$
Empty bed residence time (EBRT) (min)	$\frac{\text{Bed volume}}{\text{Volumetric flow rate of the effluent}}$
Total quantity of color adsorbed for a given C_o, Q (mg)	$q_t = QC_o \int_0^{t_t} (1 - C_t/C_o)\, dt$
Total % removal	$= q_t 1000/C_o Q t_t$
mass transfer zone (MTZ) or equivalent length of unused bed (cm)	$= H\left(1 - \frac{t_b}{t_s}\right)$

Table 3b
Effect of operating variables on a FBC design parameters

C_o (mg/L)	Q (cc/min)	H (cm)	t_t (min)	q_t (mg/g)	t_b (min)	t_s (min)	V_{eff} (mL)	EBRT (min)	Total color removal (%)	MTZ (cm)
7,693	5	5	130	28	124	7	650	3.14	24	4.74
7,693	5	15	215	65	204	11	1,075	9.42	37	14.21
7,693	5	25	380	178	361	19	1900	15.7	53	23.68
7,693	10	25	300	73	285	15	3,000	7.9	12	23.68
7,693	15	25	200	67	190	10	3,000	5.2	13	23.68
3,100	5	25	490	71	466	25	2,450	15.7	96	23.68
5,650	5	25	440	108	418	22	2,200	15.7	61	23.68

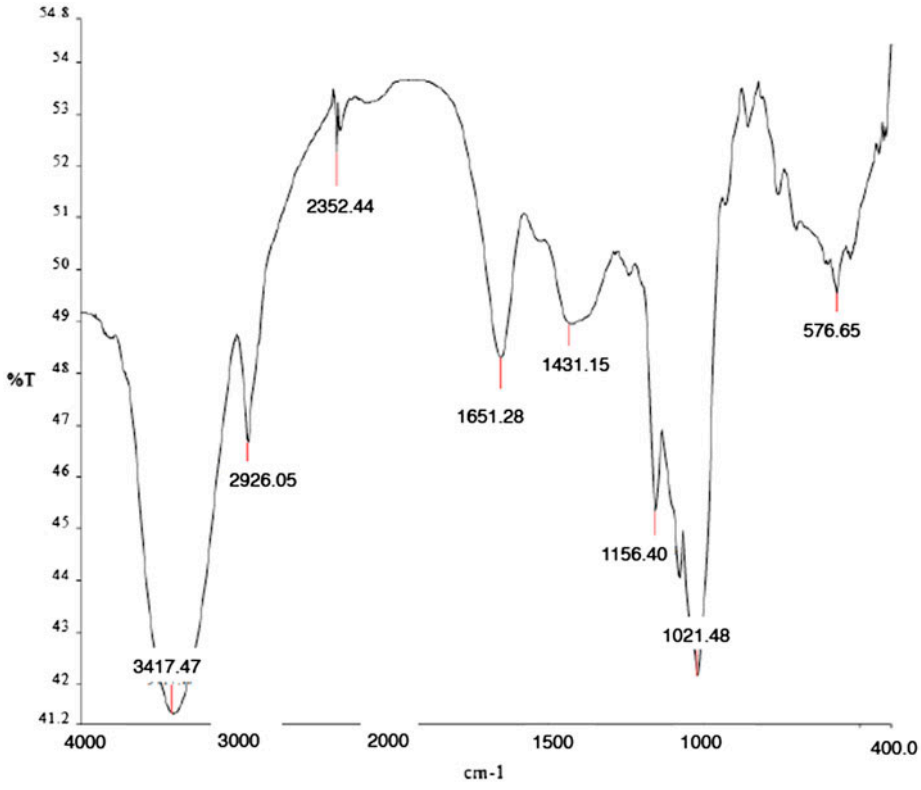

Fig. 3a. FT-IR spectrum of *S. potatorum*.

53–13% with a more rapid flow rate. Adsorption capacity was reduced from 178 to 67 mg/g and empty bed residence time fell from 15.7 to 5.2 min.

This phenomenon can be explained on the basis of mass transfer fundamentals. The rate of mass transfer went up with a higher flow rate, leading to faster saturation. Conversely, the adsorption capacity experienced a decline with augmentation of flow rate, due to shorter residence time of the adsorbate molecules in a FBC. Therefore, the surface of the adsorbent resisted saturation with the adsorbate molecules, and prevented attainment of equilibrium [22]. Mass transfer zone grew larger with enhanced flow rate. Lowering the flow rate resulted in prolonged residence time in the column. In reality, the contact time between solution and bed layer was limited, and usually insufficient for attainment of equilibrium, so it follows that when flow rate was speeded up, it was accompanied by a reduction in the volume treated efficiently until attainment of breakthrough point. Therefore, the service time of the bed also came down.

To sum up, it can be said with certainty that at a higher linear flow rate, the adsorbent got saturated quickly, because short contact time brought about

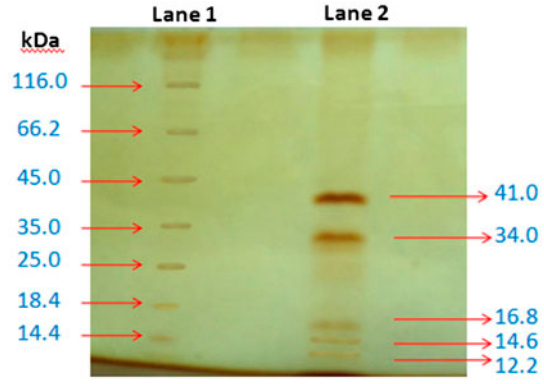

Fig. 3b. SDS-PAGE Pattern for *S. potatorum* Lane 1: Protein marker and Lane 2: *S. potatorum* seeds.

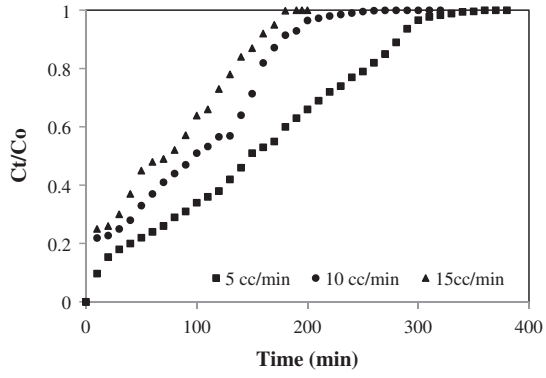

Fig. 4. Effect of inlet flow rate on color removal in a FBC Bed height: 25 cm; Flow rate: 5–15 cc/min; Initial conc.: 7,693 mg/L.

adsorption of a larger amount of pollutant on the adsorbent—the outcome was weak diffusivity of the solute amidst the adsorbent particles [24].

4.2.2. Effect of adsorbent bed height

The bed height of the adsorbent is directly proportional to the mass of the adsorbent and the availability of active sites on it. Active sites, here, refer to the sites which are responsible for the adsorption process. Bed height becomes important when designing an adsorption column to treat specific loads of pollutant in an effluent, and inadequate bed height would result in poor adsorption behavior.

Immobilized *S. potatorum* beads prepared from the sample with initial concentration of 7,693 mg/L were used for the construction of columns with bed height of 5, 15, and 25 cm (Fig. 5). The breakthrough time was observed as 124, 204, and 361 min, respectively. Total percentage removal of color for a FBC went up

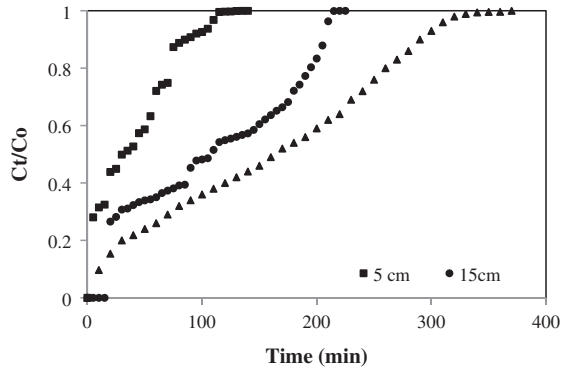

Fig. 5. Effect of bed height on color removal in a FBC Bed height: 5–25 cm; Flow rate: 5 cc/min; Initial conc.: 7,693 mg/L.

from 24 to 53% with an increase in adsorbent bed height. Values for adsorption rate (q_t) were 28, 65, and 178 mg/g, and length of mass transfer zone ascended from 4.74 to 23.68 cm. Increase in packing height delayed the empty bed residence time from 3.1 to 15.7 cm, and boosted up the volume of treated effluent from 650 to 1,900 mL (Table 3b).

The mass transfer zone in a column moves from the point of entry in the bed, and proceeds towards the exit. Hence, for the same influent concentration in a fixed-bed system, a larger bed height would mean that the mass to be transferred has to travel a longer distance to reach the exit. Consequently, an extended breakthrough time is achieved. Along the same lines, more surface area and therefore more binding sites, were available when packing volume (bed height) was greater, thereby resulting in higher uptake of effluent [25].

4.2.3. Effect of initial concentration of PIE

The three increasing levels of initial effluent concentration were 3,100, 5,650, and 7,693 mg/L. The following four parameters were reduced with rise in effluent concentration: breakthrough time (from 466 to 361 min); total time taken for adsorption (from 490 to 380 min); volume of treated water (2,450, 2,200, and 1,900 mL), and total percentage removal of color for a FBC (96, 61, and 53%). Empty bed residence time and mass transfer zone remained unaffected by changes in initial concentration, and were maintained as 15.7 min and 23.68 cm, respectively. The equilibrium color uptake was raised (71, 108, and 178 mg/g) (Table 3b, Fig. 6).

It was observed that higher initial ion concentration lowered the breakthrough time and breakthrough volume by slightly inhibiting mass-transfer flux from the bulk solution to the particle surface, probably

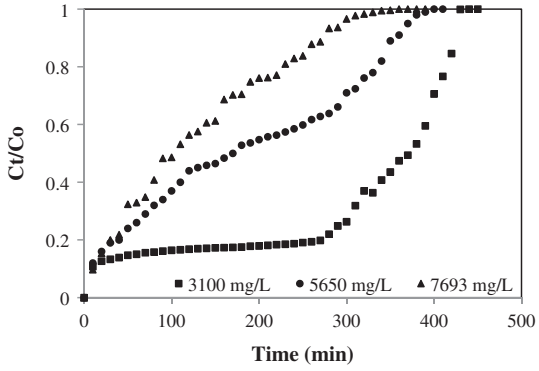

Fig. 6. Effect of initial concentration on color removal in a FBC Bed height: 25 cm; Flow rate: 5 cc/min; Initial conc.: 3,100–7,693 mg/L.

caused by weaker driving forces. Breakthrough curves became steeper as a result. Raising the concentration improved the availability of pollutant molecules for adsorption by active sites, ensuring higher uptake despite breakthrough time being shorter than at lower concentrations [26].

An increase in the initial concentration led to early saturation, bringing about speedier appearance of the breakthrough time, the reason was a reduction in transportation of mass, represented by a fall in diffusion coefficient and mass transfer coefficient at low concentrations. It was observed that at higher initial concentration of adsorbate, adsorption sites became saturated rapidly, leading to a shorter breakthrough time. Conversely, breakthrough was delayed for a lower adsorbate concentration, and adsorbent surface took a longer time to get saturated [25].

4.3. Modeling of breakthrough curves

4.3.1. BDST–Thomas model

From the slope and intercept of the linear Thomas model, it was identified that the kinetic constant k_{BDST}, and the adsorption capacity q_{BDST} is dependent on flow rate, bed height, and initial concentration. High value of regression co efficient R^2, indicates that the kinetic data confirmed well to Thomas model. With the increase in the flow rate, initial concentration, the adsorption capacity was decreased and it increased with bed height, respectively (Tables 4a–4b). The reason is that the driving force for adsorption is the concentration difference between the pollutant on the adsorbent and in the effluent. With increasing flow rate , the value of q_o decreased, because of the lower contact time between adsorbent and adsorbate. So, lower flow rate, low concentration and higher bed heights would increase the adsorption [22].

4.3.2. Adams–Bohart model

This adsorption model was applied to experimental data for the description of the initial part of the breakthrough curve. The kinetic constant k_{AB} and adsorption capacity of the adsorbent N_o was determined from the slope and intercept of the linearized plot. From Table 4b, the values of k_{AB} decreased with increase in both C_o and Q, but it increased with the increase in bed heights. This showed that the overall system kinetics was dominated by external mass transfer in the initial part of adsorption in the column [22].

Because of more saturation sites, adsorption capacity of the adsorbent N_o decreased with increasing flow rate, also, the kinetic constant k_{AB} increased with increasing flow rate [27]. This model provides a comprehensive and simple approach to running and evaluating the adsorption performance. However, its validity is limited by the range of conditions used (Table 4b).

4.3.3. Yoon–Nelson model

This model is based on the assumption that the rate of decrease in the probability of adsorption of adsorbate adsorption and the adsorbate breakthrough on the adsorbent [22]. The rate velocity constant k_{YN}, and τ is the time required for 50% adsorbate

Table 4a
Breakthrough curve models

BDST	$\ln\left[\left(\frac{C_o}{C_t}\right)-1\right] = (-k_{BDST}C_o)t + k_{BDST}\,q_{BDST}\,\frac{m}{Q}$
Yoon–Nelson model	$\ln\left(\frac{C_t}{(C_o-C_t)}\right) = k_{YN}t - k_{YN}\tau$
Adams–Bohart	$\ln\left(\frac{C_t}{C_o}\right) = (k_{AB}C_o)t - k_{AB}N_o\,\frac{H}{U_o}$
Wang	$\ln\left[1/1-\left(\frac{C_t}{C_o}\right)\right] = -k_W t + k_W t_{0.5}$

Table 4b
Parameters of breakthrough models in a FBC at various conditions

			BDST			Adams–Bohart		Yoon–Nelson				Wang		
C_o (mg/L)	Q (mL/min)	H (cm)	k_{BDST} (L/(min mg))	q_o (mg/g)	R^2	k_{AB} (L/(min mg))	N_o (mg/L)	R^2	k_{YN} (min^{-1})	τ (min)	R^2	k_W (min^{-1})	$t_{0.5}$ (min)	R^2
7,693	5	5	0.031	0.090	0.867	0.005	61	0.898	0.056	36	0.867	0.044	18	0.787
7,693	5	15	0.011	0.017	0.581	0.003	40	0.986	0.018	98	0.581	0.012	33	0.406
7,693	5	25	0.008	0.016	0.859	0.002	34	0.759	0.015	115	0.859	0.010	32	0.774
7,693	10	25	0.017	0.025	0.880	0.002	59	0.878	0.033	84	0.880	0.027	53	0.801
7,693	15	25	0.025	0.032	0.928	0.008	49	0.821	0.044	77	0.928	0.028	37	0.759
3,100	5	25	0.028	0.008	0.490	0.008	28	0.764	0.005	177	0.894	0.005	32	0.539
5,650	5	25	0.010	0.011	0.691	0.005	85	0.852	0.008	327	0.490	0.004	88	0.245

Table 5a
Mass transfer models

Weber–Morris	$q_t = k_{WM} t^{0.5} + I$
Boyd	$0.4977 + \ln\left(1 - \frac{q_t}{q_e}\right) = -Bt$; where $B = \pi^2 \frac{D_i}{r^2}$
UT	$\log\left(1 - \left(\frac{q_t}{q_e}\right)^2\right) = \left(-4\pi^2 \frac{D_i}{2.3d^2}\right)t$
Mathews–Weber	$\ln\left(\frac{C_t}{C_o}\right) = \left(-k_{MW} \frac{a}{V}\right)t$; where $\frac{a}{V} = \frac{6m}{\rho d}$

Table 5b
Parameters of mass transfer models in a FBC at various conditions

			Weber–Morris		Boyd		Urano–Tachkawa		Mathews–Weber
C_o (mg/L)	Q (cc/min)	H (cm)	k_{WM} (mg/(min$^{0.5}$ g))	R^2	D_i (cm^2/min)	R^2	D_{UT} (cm^2/min)	R^2	k_{MW} (cm/min)
7,693	5	5	0.8273	0.9683	2.01E-04	0.6567	1.92E-04	0.6354	5.04E-05
7,693	5	15	0.4339	0.9133	3.12E-05	0.561	5.51E-05	0.6297	5.89E-06
7,693	5	25	0.9446	0.9837	6.81E-05	0.6756	1.13E-04	0.6613	1.15E-06
7,693	10	25	0.6053	0.9450	1.32E-04	0.6583	3.33E-06	0.7865	2.29E-05
7,693	15	25	0.5855	0.9450	1.24E-04	0.5683	3.05E-04	0.6659	4.81E-05
3,100	5	25	0.1248	0.8771	2.90E-05	0.4161	4.93E-05	0.3885	1.53E-06
5,650	5	25	0.1959	0.4772	7.03E-05	0.6962	2.61E-06	0.6732	4.33E-06

breakthrough were calculated. k_{YN} was higher at higher flow rate, higher initial concentration, and lower bed height. Also, τ, time required for 50% adsorbate breakthrough decreased with increase in flow rate, C_o, and decreased with the increase in H (Table 4b). This is due to the fact that increase in initial concentration increases the competition between adsorbate molecules for the adsorption site, which ultimately results in increased uptake ratio [26].

4.3.4. Wang model

Wang model is a mass transfer model used to describe the breakthrough curve of solutions containing pollutant in the fixed bed on the basis of the following assumptions (i) The adsorption process remains isothermal (ii) The breakthrough curve is symmetrical, and, (iii) There is negligible axial dispersion in the column. A plot of ln $[1/(1 - (C_t/C_o)]$ vs. t produces the slope and intercept value as $1/k_w$ and $t_{0.5}$, respectively, where k_w is the kinetic constant. Meanwhile, similar to the Yoon–Nelson model, it cannot provide sufficient information of an adsorption system [28] (Table 4b).

4.4. Mass transfer mechanism

The significance of diffusion mechanisms and accurate estimates of the diffusivities inside the adsorbent particles are determined from the diffusion-controlled kinetic models, based on interpretation of the experimental data (Table 5a) [29].

4.4.1. Weber–Morris model

In the adsorption process besides adsorption to the surface, mass may also transfer due to intra-particle diffusion. The model was developed by Weber–Morris based on intra-particle diffusion. According to this model, a plot of solute adsorbed against the square root of the contact time should yield a straight line passing through the origin. k_{WM} is the intra-particle diffusion rate constant. When the plot does not pass through the origin, then it gives an indication of some degree of film diffusion control and intra-particle diffusion is not only the rate-limiting step. In this case, the plot is not passing through origin, indicating that the intra-particle diffusion was not only the rate-controlling step, film diffusion was also expected to affect the adsorption. The larger the k_{WM} values, the easier the diffusion and transport into the pores of adsorbents. The value of intercept I gives an idea about the boundary layer thickness, i.e. the larger intercept, the greater the boundary layer effect [30]. It is indicating that the effects of mass transfer resistance on the adsorbate were gradually higher. Hence, the external mass transfer resistance could not be ignored (Table 5b).

4.4.2. Boyd model

A clear difference between the film and particle diffusion has to be made for the purpose of understanding the adsorption mechanism. Boyd model is used for film diffusion, and to test the linearity of the experimental values, with a plot of $[-0.4997 - \ln(1 - F)]$ against time.

It can be hypothesized that the decolorization of PIE was mainly governed by the external mass transport where intra-particle diffusion was the rate-limiting step [31]. To determine whether the adsorption process occurred by external diffusion or intra-particle mechanism, the kinetic data were analyzed with the help of the Boyd model [32]. The presence of an intercept showed that diffusion was not the only observed mechanism of transfer. A linear plot, with its slope equal to B, would mean that pore diffusion is the rate-controlling step. The effective diffusion coefficient, D_i (cm^2/s) was calculated from this (Table 5b). Linear segments can also be encountered in Boyd plots, and in such cases, every segment is analyzed separately to arrive at the corresponding diffusion coefficient. The observation of an intercept is predictive of a second mass transfer mechanism (external mass transfer) [33].

4.4.3. Urano–Tachikawa model

Urano–Tachkawa intra-particular mass transfer diffusion equation is used to describe the kinetic data of color adsorption onto immobilized natural adsorbents. The dependence of $F(q_t/q_e)$ on t is plotted in a linear form. The constant of the internal diffusion is determined from the slopes of the lines [34] and listed in Table 5b.

Due to the increase in the volumetric flow rate, the diffusivity of the sorbate into the sorbent increased. The pollutant load was greater in the case of effluents with higher initial concentration, because of the increased concentration gradient; the diffusivity was in ascending nature with increase in initial concentrations. Earlier workers [35] in this field reported D_{UT} values in the range of 10^{-12}–10^{-13} cm^2/s for intra-particle diffusion to be the rate-limiting step for the adsorption of organic compounds. As per this postulation, the rate-limiting step appeared to be particle diffusion since the D_{UT} values were in the order of 10^{-12} cm^2/s. The adsorption process could be best explained by the Urano–Tachikawa equation, indicating the controlling nature of intra-particle diffusion.

4.4.4. Mathews–Weber model

The external mass transfer coefficients for the adsorption could be determined by Mathews–Weber model. It expresses the evolution of the concentration of the solute in the solution (Table 5b).The significance of diffusion mechanisms and accurate estimation of the diffusivities inside the adsorbent particles were determined from the diffusion-controlled kinetic models based on interpretation of the experimental data. The external diffusion model assumed that the concentration at the adsorbent surface tended towards zero and the intra-particle diffusion was negligible at early contact time.

The k_{MW} values decreased with increase in the initial dye concentrations, indicating that the external mass transfer rate is slower at higher initial dye concentration. The velocity of dye transport from liquid phase to solid phase decreased but the intra-particle diffusion increased with increase in the initial dye concentrations [30].

5. Conclusions

It was found that these natural materials, *S. potatorum*, could be incorporated into the matrix of sodium alginate. The percentage color removal from PIE was found to rise with an increase in the bed height, and fall with an increase in flow rate and initial concentration. The presence of a large number of actives sites (due to larger bed height), higher mass transfer gradient (due to higher initial concentration), and larger residence time (due to lower flow rate) resulted in a higher adsorption capacity. Breakthrough curves were fitted with the curves of Thomas–Bed depth service time (BDST) model, Adams–Bohart model, Yoon–Nelson model, and Wang model. Adsorption capacity, kinetic rate constants, and time required for 50% adsorbate breakthrough were enumerated from model parameters.

To understand the transport of pollutant ions onto the immobilized beads of adsorbents, and to identify the rate-limiting steps of the overall adsorption process, the following mass transfer models were performed: Weber–Morris model, Boyd model, Urano–Tachkawa model and Mathews–Weber model.

(1) Through the results of Weber–Morris model, it was noted that the intra-particle diffusion was not the only rate-controlling step, but film diffusion was also a likely influencing factor.

(2) The Boyd model gave rise to linear plots (which however did not pass through the origin), implying that the process is not only the film diffusion controlled.
(3) The diffusion constants of Urano–Tachkawa model were in the medium range (10^{-5}) which indicates that intra-particle diffusion was not the only rate-controlling step.
(4) The mass transfer co efficient of the Mathews–Weber model were in the medium range of 10^{-5}, which implies that the film diffusion was not only the rate-controlling step.

This investigation showed that the environmental friendly, agro-based material *S. potatorum* was a promising adsorbent in the removal of color from water-based PIE using fixed-bed column. It was found that these results support the applicability of this adsorbent in PIE treatment. The determined column parameters can be scaled up for the design of a FBC.

Nomenclature

a	—	total interfacial area of particle (cm^2)
C_o, C_t	—	concentration of the solute at initial time and time 't' in the effluent (mg/L)
d	—	mean diameter of immobilized beads (cm)
D_{UT}	—	Diffusion constant in Urano–Tachkawa model (cm^2/min)
H	—	bed height (cm)
I	—	thickness of boundary layer (mg/g)
k_{AB}	—	kinetic constant in the Adams–Bohart model (L/(min mg))
k_{BDST}	—	kinetic constant in the BDST model (L/(min mg))
k_{MW}	—	external mass transfer coefficient in Mathews–Weber model (cm/min)
k_W	—	kinetic constant in the Wang model (1/min)
k_{WM}	—	kinetic constant in the Weber–Morris model (mg/($min^{0.5}$ g))
k_{YN}	—	kinetic constant in the Yoon–Nelson model (1/min)
m	—	total mass of an adsorbent (g)
N_o	—	maximum adsorption capacity per unit volume of adsorption column (mg/L)
Q	—	inlet feed flow rate (mL/min)
q_{BDST}	—	maximum adsorption in BDST model (mg/g)
q_t, q_e	—	total adsorbed quantity of color in the column and at exhaustion time (mg/g)
r	—	Mean radius of an immobilized adsorbent beads (cm)
R^2	—	correlation coefficient
t, t_b, t_s, t_t	—	time, breakthrough time, saturation time, and total time taken in a FBC (min)
$t_{0.5}$	—	time required for 50% adsorbate breakthrough time (min)
U_o	—	linear velocity of inlet effluent (cm/min)
V, V_{eff}	—	volume of effluent, and volume of effluent treated (mL)
τ	—	time required for 50% adsorbate breakthrough time in Yoon–Nelson model(min)
ρ	—	apparent density of the adsorbent (g/mL)

References

[1] B.K. Körbahti, N. Aktaş, A. Tanyolaç, Optimization of electrochemical treatment of industrial paint wastewater with response surface methodology, J. Hazard. Mater. 148 (2007) 83–90.
[2] A.E. Mohsen, M. Hassanin M. Kamel, Appropriate technology for industrial wastewater treatment of paint industry, Am.–Eurasian J. Agric. Environ. 8(5) (2010) 597–601.
[3] C.P. Haung, M. Ghadirian, Physical-Chemical treatment of paint industry wastewater, J. Water Pollut. Control Fed. 46(10) (1974) 2340–2346.
[4] J.A. Brown, M. Weintraub, Bio oxidation of paint process wastewater, J. Water Pollut. Control Fed. 54(7) (1982) 1127–1130.
[5] M.C. Arquiaga, L.W. Canter, J.M. Robertson, Microbiological characterization of the biological treatment of aircraft paint stripping wastewater, Environ. Pollut. 89 (2) (1995) 189–195.
[6] S. Shanta, S.N. Kaul, Performance of evaluation of a pure oxygen-based activated sludge system treatment a combined paint industry wastewater and domestic sewage, Int. J. Environ. Stud. 58(4) (2000) 445–457.
[7] B. Sengupta, B.K. Dey, M.A. Hashim, S. Hasan, Micro filtration of water-based paint effluents, Int. J. Environ. Manage. 8(3–4) (2004) 455–466.
[8] S. Vishali, R. Karthikeyan, *Cactus opuntia* (*ficus-indica*): An eco-friendly alternative coagulant in the treatment of paint effluent, Desalin. Water Treat. (2014), doi:10.1080/19443994.2014.945487.
[9] J.M. Xiang, L.X. Hui, Treatment of water based printing ink wastewater by Fenton process combined with coagulation, J. Hazard. Mater. 162 (2009) 386–390.
[10] M.Y. Pamukoglu, F. Kargi, Removal of copper(II) ions from aqueous medium by biosorption onto powdered waste sludge, Process Biochem. 41(5) (2006) 1047–1054.
[11] B.K. Körbahti, A. Tanyolac, Electrochemical treatment of simulated industrial paint wastewater in a continuous tubular reactor, Chem. Eng. J. 148(2–3) (2009) 444–451.

[12] A. Akyol, Treatment of paint manufacturing wastewater by electrocoagulation, Desalination 285(31) (2012) 91–99.
[13] G.L. Dotto, E.C. Lima, L.A.A. Pinto, Biosorption of food dyes onto *Spirulina platensis* nanoparticles: Equilibrium isotherm and thermodynamic analysis, Bioresour. Technol. 103 (2012) 123–130.
[14] S. Dahiya, R.M. Tripathi, A.G. Hegde, Biosorption of lead and copper from aqueous solutions by pre-treated crab and arca shell biomass, Bioresour. Technol. 8 (99) (2008) 179–187.
[15] S. Vishali, R. Karthikeyan, A comparative study of *Strychnos potatorum* and chemical coagulants in the treatment of paint and industrial effluents: An alternate solution, Sep. Sci. Technol. 49(16) (2014) 2510–2517.
[16] R. Babu, M. Chaudhri, Home water treatment by direct filtration with natural coagulant, J. Water Health 03(1) (2005) 27–30.
[17] G. Muthuraman, S. Sasikala, Removal of turbidity from drinking water using natural coagulants, J. Ind. Eng. Chem. 20 (2014) 1727–1731.
[18] K. Jayaram, I.Y.L.N. Murthy, H. Lalhruaitluanga, M.N.V. Prasad, Biosorption of lead from aqueous solution by seed powder of *Strychnos potatorum* L, Colloids Surf., B: Biointerfaces 71(2) (2009) 248–254.
[19] P. Senthil Kumar, C. Senthamarai, A.S.L. Sai Deepthi, R. Bharan, Adsorption isotherms, kinetics and mechanism of Pb(II) ions removal from aqueous solution using chemically modified agricultural waste, Can. J. Chem. Eng. 9999 (2013) 1–7.
[20] R. Kannan, S. Lakshmi, P. Radha, N. Aparna, S. Vishali, W.R. Thilagaraj, Biosorption of heavy metals from actual electroplating wastewater using encapsulated *Moringa oleifera* beads in fixed bed column, Desalin. Water Treat. (2014), doi:10.1080/19443994.2014.985725.
[21] S. XiaoFeng, T. Imai, M. Sekine, H. Takaya, Y. Koichi, K. Ariyo, N.A. Shiori, Adsorption of phosphate using calcined Mg_3-Fe layered double hydroxides in a fixed bed column study, J. Ind. Eng. Chem. 20 (2014) 3623–3630.
[22] A.A. Ahmad, B.H. Hameed, Fixed bed adsorption of reactive azo dye onto granular activated carbon prepared from waste, J. Hazard. Mater. 175 (2010) 298–303.
[23] M.M.S. Saif, N. Siva Kumar, M.N.V. Prasad, Binding of cadmium to *Strychnos potatorum* seed proteins in aqueous solution: Adsorption kinetics and relevance to water purification, Colloids Surf., B: Biointerfaces 94 (2012) 73–79.
[24] X. Luo, Z. Deng, X. Lin, C. Zhang, Fixed bed column study for Cu^{2+} removal from solution using expanding rice husk, J. Hazard. Mater. 187 (2011) 182–189.
[25] Z.Z. Chowdhury, S.M. Zain, A.K. Rashid, R.F. Rafique, K. Khalid, Breakthrough curve analysis for column dynamics sorption of Mn(II) ions from wastewater by using *Mangostana garcinia* Peel-based granular activated carbon J. Chem. (2013) 1–8. Available from: http://dx.doi.org/10.1155/2013/959761.
[26] J.T. Nwabanne, P.K. Igbokwe, Adsorption of packed bed column for the removal of lead(II) using oil palm fibre, Int. J. Appl. Sci. Technol. 2(5) (2012) 106–115.
[27] S. Zahra, S. Reyhane, F. Reza, Fixed-bed adsorption dynamics of Pb(II) adsorption from aqueous solution using nanostructured γ-alumina, J. Nanostruct. Chem. 3(48) (2013) 1–8.
[28] Z. Xu, J.G. Cai, B.C. Pan, Mathematically modeling fixed-bed adsorption in aqueous systems, J. Zhejiang Univ. Sci. A 14(3) (2013) 155–176.
[29] R. Krishna Prasad, S.N. Srivatava, Sorption of distillery spent wash onto fly ash: Kinetics, mechanism, process design and factorial design, J. Hazard. Mater. 161 (2–3) (2009) 1313–1322.
[30] E.W. Bao, Y.H. Yong, X. Lei, P. Kang, Biosorption behavior of azo dye by inactive CMC immobilized *Aspergillus fumigates* beads, Bioresour. Technol. 99 (2008) 794–800.
[31] A.O. Okewale, P.K. Igbokwe, J.O. Ogbuagu, Kinetics and isotherm studies of the adsorptive dehydration of ethanol-water system with biomass based materials, Int. J. Eng. Innov. Technol. 2(9) (2013) 36–42.
[32] R.N.P. Teixera, V.O.S. Neto, J.T. Oliveira, T.C. Oliveira, D.Q. Melo, M.A.A. Silva, R.F. Nascimento, Study on the use of roasted barley powder for adsorption of Cu^{2+} ions in batch experiments and in fixed bed columns, Bioresources 8(3) (2013) 3556–3573.
[33] I.E. Hristova, Comparison of different kinetic models for adsorption of heavy metals onto activated carbon from apricot stones, Bulg. Chem. Commun. 43 (2011) 370–377.
[34] Y. Sağ, Y. Aktay, Mass transfer and equilibrium studies for the sorption of chromium ions onto chitin, Process Biochem. 36 (2000) 157–173.
[35] V.P. Vinod, T.S. Anirudhan, Adsorption behavior of basic dyes on the humic acid immobilized pillared clay, Water Air and Soil Pollut. 150 (2003) 193–217.